Structural Characterization and Formation Kinetics of Sitting-Atop (SAT) Complexes of Some Porphyrins with Copper(II) Ion in Aqueous Acetonitrile Relevant to Porphyrin Metalation Mechanism. Structures of Aquacopper(II) and Cu(II)−SAT Complexes As Determined by XAFS Spectroscopy

Masahiko Inamo,[†] Naruhisa Kamiya,[†] Yasuhiro Inada,[‡] Masaharu Nomura,[§] and Shigenobu Funahashi*,[⊥]

Department of Chemistry, Aichi University of Education, Igaya, Kariya 448-8542, Japan, Research Center for Materials Science, Nagoya University, Chikusa, Nagoya 464-8602, Japan, Photon Factory, Institute of Materials Structure Science, High Energy Accelerator Research Organization, Oho, Tsukuba 305-0801, Japan, and Laboratory of Analytical Chemistry, Graduate School of Science, Nagoya University, Chikusa, Nagoya 464-8602, Japan

The formation of the sitting-atop (SAT) complexes of 5,10,15,20-tetraphenylporphyrin (H_2tpp), 5,10,15,20-tetrakis-(4-chlorophenyl)porphyrin (H_2t(4-Clp)p), 5,10,15,20-tetramesitylporphyrin (H_2tmp), and 2,3,7,8,12,13,17,18-octaethylporphyrin (H_2oep) with the Cu(II) ion was spectrophotometrically confirmed in aqueous acetonitrile (AN), and the formation rates were determined as a function of the water concentration (C_W). The decrease in the conditional first-order rate constants with the increasing C_W was reproduced by taking into consideration the contribution of $[Cu(H_2O)(an)_5]^{2+}$ in addition to $[Cu(an)_6]^{2+}$ to form the Cu(II)−SAT complexes. The second-order rate constants for the reaction of $[Cu(an)_6]^{2+}$ and $[Cu(H_2O)(an)_5]^{2+}$ at 298 K were respectively determined as follows: $(4.1 \pm 0.2) \times 10^5$ and $(3.6 \pm 0.2) \times 10^4$ M^{-1} s^{-1} for H_2tpp, $(1.15 \pm 0.06) \times 10^5$ M^{-1} s^{-1} and negligible for H_2t(4-Clp)p, and $(4.8 \pm 0.3) \times 10^3$ and $(1.3 \pm 0.3) \times 10^2$ M^{-1} s^{-1} for H_2tmp. Since the reaction of H_2oep was too fast to observe the reaction trace due to the dead time of 2 ms for the present stopped-flow technique, the rate constant was estimated to be greater than 1.5×10^6 M^{-1} s^{-1}. According to the structure of the Cu(II)−SAT complexes determined by the fluorescent XAFS measurements, two pyrrolenine nitrogens of the *meso*-substituted porphyrins (H_2tpp and H_2tmp) bind to the Cu(II) ion with a Cu−N(pyr) distance of ca. 2.04 Å, while those of the *β*-pyrrole-substituted porphyrin (H_2oep) coordinate with the corresponding bond distance of 1.97 Å. The shorter distance of H_2oep is ascribed to the flexibility of the porphyrin ring, and the much greater rate for the formation of the Cu(II)−SAT complex of H_2oep than those for the *meso*-substituted porphyrins is interpreted as due to a small energetic loss at the porphyrin deformation step during the formation of the Cu(II)−SAT complex. The overall formation constants, β_n, of $[Cu(H_2O)_n(an)_{6-n}]^{2+}$ for the water addition in aqueous AN were spectrophotometrically determined at 298 K as follows: $\log(\beta_1/M^{-1}) = 1.19 \pm 0.18$, $\log(\beta_2/M^{-2}) = 1.86 \pm 0.35$, and $\log(\beta_3/M^{-3}) = 2.12 \pm 0.57$. The structure parameters around the Cu(II) ion in $[Cu(H_2O)_n(an)_{6-n}]^{2+}$ were determined using XAFS spectroscopy.

Introduction

The formation mechanisms of metalloporphyrins have been extensively investigated since the sitting-atop (SAT) intermediate was suggested to exist during the metalation process by Fleisher and Wang.[1] In this so-called SAT complex, two pyrrolenine nitrogens of the porphyrin coordinate to the metal ion, and two protons on the pyrrole nitrogens still remain. Recently, the SAT complex of 5,10,15,20-tetraphenylporphyrin (H_2tpp) was successfully detected during the reaction with the Cu(II) ion in acetonitrile (AN).[2,3] The very low Brønsted basicity of AN forces the pyrrole protons of H_2tpp to rest in the reaction product, the Cu(II)−SAT complex. Furthermore, the existence and the rate-determining formation of the Cu(II)−SAT complex during the metalation of H_2tpp with the Cu(II) ion have been kinetically demonstrated by adding pyridine (py) as a proton acceptor to stabilize the released protons.[2] It was revealed by independent measurements of the deprotonation rate of the Cu(II)−SAT complex in AN that the deprotonation of the Cu(II)−SAT complex to form the metalloporphyrin, [Cu(tpp)], is promoted by the nucleophilic attack of the Brønsted base as a proton acceptor on the pyrrole proton, and that the deprotonation rate is proportional to the basicity of the Brønsted base.[4] The SAT complexes of H_2tpp with several 3d-block cations in AN have also been evaluated, and the characteristics of their UV−vis absorption spectra have been shown to depend on the number of d electrons and the size of the metal(II) ion.[5] According to these results obtained by the strategic use of AN as a solvent with very weak basicity, the overall metalation

* To whom correspondence should be addressed. E-mail: sfuna@chem4.chem.nagoya-u.ac.jp.
† Aichi University of Education.
‡ Research Center for Materials Science, Nagoya University.
§ Institute of Materials Structure Science.
⊥ Laboratory of Analytical Chemistry, Nagoya University.

(1) Fleischer, E. B.; Wang, J. H. *J. Am. Chem. Soc.* **1960**, *82*, 3498.
(2) Inada, Y.; Sugimoto, Y.; Nakano, Y.; Itoh, Y.; Funahashi, S. *Inorg. Chem.* **1998**, *37*, 5519.
(3) Inada, Y.; Sugimoto, Y.; Nakano, Y.; Funahashi, S. *Chem. Lett.* **1996**, 881.
(4) Inada, Y.; Yamaguchi, T.; Satoh, H.; Funahashi, S. *Inorg. React. Mech.* **2000**, *2*, 277.
(5) Inada, Y.; Nakano, Y.; Inamo, M.; Nomura, M.; Funahashi, S. *Inorg. Chem.* **2000**, *39*, 4793.

10.1021/ic010162b CCC: $20.00
Published on Web 09/28/2001

reaction of H_2tpp with an octahedrally solvated metal(II) ion (MS_6^{2+}) in the conventional basic solvent (S) was resolved into eqs 1−6 which follow: the deformation of the porphyrin ring (eq 1), the outer-sphere association (eq 2), the rate-determining exchange of a coordinated solvent molecule with a first pyrrolenine nitrogen (eq 3), the chelate ring closure to form the SAT complex (eq 4), the first deprotonation on the pyrrole nitrogen in the SAT complex by the basic solvent molecule (*S*) (eq 5), and the second deprotonation to form the metalloporphyrin (eq 6),

$$H_2\text{tpp} \overset{K_D}{\rightleftharpoons} H_2tpp \quad (1)$$

$$H_2tpp + MS_6^{2+} \overset{K_{OS}}{\rightleftharpoons} H_2tpp{\cdot}MS_6^{2+} \quad (2)$$

$$H_2tpp{\cdot}MS_6^{2+} \underset{k_{-1}}{\overset{k_1}{\rightleftharpoons}} MS_5(H_2\text{tpp})^{2+} + S \quad (3)$$

$$MS_5(H_2\text{tpp})^{2+} \overset{K_{RC}}{\rightleftharpoons} MS_p(H_2\text{tpp})^{2+} + (5-p)S \quad (4)$$

$$MS_p(H_2\text{tpp})^{2+} + S \overset{K_{-H1}}{\rightleftharpoons} MS_q(\text{Htpp})^{+} + HS^{+} + (p-q)S \quad (5)$$

$$MS_q(\text{Htpp})^{+} + S \overset{K_{-H2}}{\rightleftharpoons} MS_r(\text{tpp}) + HS^{+} + (q-r)S \quad (6)$$

where $p \leq 4$, $q \leq p - 1$, and $r \leq 2$. In the case of M = Cu, S = AN, and S = py, it was determined by fluorescent XAFS measurements that $p = 4$ and $r = 0$.[4] The reaction scheme described by eqs 1−6 can well explain the previously observed results, such as the parallel dependence of the metalation rate constant on the solvent exchange rate constant of MS_6^{2+},[6−12] the increase in the metalation rate for the nonplanar porphyrins,[11−16] the dependence of the metalation rate on the Brønsted basicity of the free porphyrins,[16−18] the $[H^+]^2$-dependent rate law for the demetalation in aqueous solution,[19−22] and the dependence of the metalation rate constant on the ionic strength for the charged porphyrins.[23]

In this study, we have extended the structural and kinetic investigation on the Cu(II)−SAT complex to some other systems with some porphyrins (H_2por), such as 5,10,15,20-tetrakis(4-chlorophenyl)porphyrin (H_2t(4-Clp)p), 5,10,15,20-tetramesitylporphyrin (H_2tmp), and 2,3,7,8,12,13,17,18-octaethylporphyrin (H_2oep). The structures of these porphyrins are shown in Scheme 1. H_2tpp is a typical *meso*-substituted porphyrin. The

Scheme 1

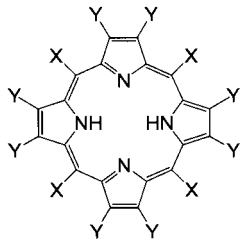

	X	Y
H_2tpp		H
H_2t(4-Clp)p		H
H_2tmp		H
H_2oep	H	C_2H_5

electron density and the donating ability of the pyrrolenine nitrogen, which is the first bonding atom toward the metal ion in the SAT complex formation process, are considered to be lowered in the case of H_2t(4-Clp)p containing electron-withdrawing chlorine atoms. The bulkiness of the *meso*-substituents is augmented for H_2tmp. Furthermore, the examination will provide an evaluation of the difference in reactivity and structure due to the difference in the substituted site. The structural and kinetic investigations using a variety of porphyrins will provide significant information on the SAT complex formation mechanism to propose the general metalation mechanism of the porphyrins.

The previous study has indicated that the formation rate of the Cu(II)−SAT complex of H_2tpp decreases with the increasing concentration of py added to the solution as a proton acceptor.[2] The decrease was interpreted in terms of the lower reactivity of the py-substituted Cu(II) species compared to the fully AN-solvated species, and it was interpreted as due to the intramolecular axial−equatorial (ax−eq) interconversion of the Cu(II) ion. In this study, we have used water instead of py as a substituting ligand of the Cu(II) ion, and the Cu(II)−SAT complex formation rates have been measured in aqueous AN by varying the water concentration. Because the formation constants of the water-substituted Cu(II) ion in AN, $[Cu(H_2O)_n(an)_{6-n}]^{2+}$, are necessary to speciate the reacting Cu(II) species, the values of the formation constants have also been spectrophotometrically determined. Furthermore, the local structure around the Cu(II) ion in the $[Cu(H_2O)_n(an)_{6-n}]^{2+}$ complexes was clarified using XAFS spectroscopy to determine the structural characteristics of the reacting Cu(II) species. The rate constants of the Cu(II)−SAT complex formation for $[Cu(H_2O)_n(an)_{6-n}]^{2+}$ are quite useful in understanding the substitution mechanism on the labile Cu(II) ion by comparing the corresponding values of $[Cu(py)_n(an)_{6-n}]^{2+}$ reported earlier.[2] Although the dissociative interchange of the solvent molecule was evaluated at the elongated axial site of the solvated Cu(II) ion in some solvents via the fast ax−eq interconversion,[24−29] the studies on the complexation rates of the solvated Cu(II) ion are rare because the ligand substitution is quite fast due to the labilized axial site. The deformation process of the porphyrin (eq 1) requires an energetic loss prior to the formation of the Cu(II)−SAT complex, and thus the measurement of the reaction rates on the solvated Cu(II) ion is possible using a conventional stopped-flow technique. Such a kinetic observation is a great

(6) Hambright, P.; Chock, P. B. *J. Am. Chem. Soc.* **1974**, *96*, 3123.
(7) Turay, J.; Hambright, P. *Inorg. Chem.* **1980**, *19*, 562.
(8) Choi, E. I.; Fleischer, E. B. *Inorg. Chem.* **1963**, *2*, 94.
(9) Fleischer, E. B.; Choi, E. I.; Hambright, P.; Stone, A. *Inorg. Chem.* **1964**, *3*, 1284.
(10) Kingham, D. J.; Brisbin, D. A. *Inorg. Chem.* **1970**, *9*, 2034.
(11) B.-Ackerman, M. J.; Lavallee, D. K. *Inorg. Chem.* **1979**, *18*, 3358.
(12) Funahashi, S.; Yamaguchi, Y.; Tanaka, M. *Inorg. Chem.* **1984**, *23*, 2249.
(13) Funahashi, S.; Ito, Y.; Kakito, H.; Inamo, M.; Hamada, Y.; Tanaka, M. *Mikrochim. Acta* **1986**, 33.
(14) Funahashi, S.; Yamaguchi, Y.; Tanaka, M. *Bull. Chem. Soc. Jpn.* **1984**, *57*, 204.
(15) Shah, B.; Shears, B.; Hambright, P. *Inorg. Chem.* **1971**, *10*, 1828.
(16) Robinson, L. R.; Hambright, P. *Inorg. Chim. Acta* **1991**, *185*, 17.
(17) Reid, J. B.; Hambright, P. *Inorg. Chem.* **1977**, *16*, 968.
(18) Shamim, A.; Hambright, P. *Inorg. Chem.* **1980**, *19*, 564.
(19) Inamo, M.; Tomita, A.; Inagaki, Y.; Asano, N.; Suenaga, K.; Tabata, M.; Funahashi, S. *Inorg. Chim. Acta* **1997**, *256*, 77.
(20) Shears, B.; Shah, B.; Hambright, P. *J. Am. Chem. Soc.* **1971**, *93*, 776.
(21) Tabata, M.; Oshita, K.; Tanaka, M. *Mikrochim. Acta* **1985**, 397.
(22) Rahimi, R.; Sutter, T. P. G.; Hambright, P. *J. Coord. Chem.* **1995**, *34*, 283.
(23) Nwaeme, J.; Hambright, P. *Inorg. Chem.* **1984**, *23*, 1990.
(24) Swift, T. J.; Connick, R. E. *J. Chem. Phys.* **1962**, *37*, 307.
(25) Powell, D. H.; Helm, L.; Merbach, A. E. *J. Chem. Phys.* **1991**, *95*, 9258.
(26) Powell, D. H.; Furrer, P.; Pittet, P.-A.; Merbach, A. E. *J. Phys. Chem.* **1995**, *99*, 16622.
(27) Poupko, R.; Luz, Z. *J. Chem. Phys.* **1972**, *57*, 3311.
(28) Helm, L.; Lincoln, S. F.; Merbach, A. E. *Inorg. Chem.* **1986**, *25*, 2550.
(29) Inada, Y.; Ozustumi, K.; Funahashi, S.; Soyama, S.; Kawashima, T.; Tanaka, M. *Inorg. Chem.* **1993**, *32*, 3010.

help for evaluating the complexation mechanism on the Cu(II) ion, and the comparison of the Cu(II)−SAT complex formation rates between the $[Cu(L)_n(an)_{6-n}]^{2+}$ (L = water in this study and py previously reported) complexes will clarify the ligand substitution mechanism on the Cu(II) ion with an asymmetrical environment which has never been investigated as far as we know.

In this article, we will discuss the formation mechanism of the Cu(II)−SAT complexes for four porphyrins relevant to the total mechanism of the porphyrin metalation, and we will argue the ligand substitution mechanism of the Cu(II) ion with an asymmetrical coordination environment on the basis of the kinetic and structural results regarding the Cu(II)−SAT complexes.

Experimental Section

Materials. Acetonitrile (Wako Pure Chemical Co., Japan) was dried over activated 4 Å molecular sieves for several days and was distilled at 110 °C under a nitrogen atmosphere. H_2tpp (Dojin Lab., Japan) and H_2oep (Dojin) were used without further purification. H_2t(4-Clp)p was synthesized from 4-chlorobenzaldehyde and pyrrole by a method similar to that used for H_2tpp.[30,31] H_2tmp was synthesized according to the literature method.[32] $Cu(CF_3SO_3)_2$ was prepared according to the method previously reported.[2] Doubly distilled water was used for the preparation of the aqueous acetonitrile solutions.

Preparation of Sample Solutions. Sample solutions for all of the measurements were prepared by dissolving an adequate amount of $Cu(CF_3SO_3)_2$ or porphyrins in aqueous AN. The water concentration in the sample solutions was measured by the Karl−Fisher method (CA-06, Mitsubishi Chemical, Japan). The concentrations of the sample solutions for the spectrophotometric measurements, the XAFS measurements in the transmission mode, and the fluorescent XAFS measurements are summarized in Tables S1−S3 (Supporting Information).

Spectrophotometric Measurements and Data Analysis. To determine the formation constants of $[Cu(H_2O)_n(an)_{6-n}]^{2+}$ for the water addition reaction in AN, the UV−vis absorption spectra of the AN solutions containing both the Cu(II) ion and water were measured using a UV−vis spectrophotometer (U-3000, Hitachi, Japan) over the wavelength range from 250 to 860 nm at 25.0 ± 0.1 °C. All of the observed absorption spectra are given in Figure S1.

The spectral data were analyzed by a least-squares calculation on the basis of eq 7,

$$A_\lambda = \sum_n \epsilon_{Cu(H_2O)_n,\lambda}[Cu(H_2O)_n(an)_{6-n}{}^{2+}] \quad (7)$$

where A_λ is the absorbance at wavelength λ and $\epsilon_{Cu(H_2O)_n,\lambda}$ is the molar absorption coefficient of $[Cu(H_2O)_n(an)_{6-n}]^{2+}$ at wavelength λ. Total concentrations of the Cu(II) ion (C_{Cu}) and water (C_W) are respectively given by eqs 8 and 9,

$$C_{Cu} = [Cu(an)_6{}^{2+}] + \sum_n \beta_n [Cu(an)_6{}^{2+}]\,[H_2O]^n \quad (8)$$

$$C_W = [H_2O] + \sum_n n\beta_n [Cu(an)_6{}^{2+}]\,[H_2O]^n \quad (9)$$

where β_n is the overall formation constant of the $[Cu(H_2O)_n(an)_{6-n}]^{2+}$ complex defined as $\beta_n = [Cu(H_2O)_n(an)_{6-n}{}^{2+}]\,[Cu(an)_6{}^{2+}]^{-1}\,[H_2O]^{-n}$. The least-squares calculation was carried out by optimizing the values of β_n and $\epsilon_{Cu(H_2O)_n,\lambda}$ using the program MQSPEC.[33] The A_λ values at 38 wavelengths were used in the calculation.

XAFS Measurements and Data Analysis. The XAFS spectra in the vicinity of the Cu K edge were measured at the BL-12C station of the Photon Factory of the High Energy Acceleration Research Organization.[34−36] The incident and transmitted X-ray intensities were measured by ionization chambers with lengths of 17 and 31 cm and filled with N_2 gas and a 3:17 mixture of Ar and N_2 gas, respectively. In the case of the fluorescent XAFS measurements, the fluorescent X-ray intensity was measured using a 19-element solid-state detector (SSD).[35,36] The shaping time of the spectroscopy amplifier was 0.25 μs. The white synchrotron radiation was monochromatized by an Si(111) double crystal which was detuned to 80% of the maximal intensity at the K edge of Cu. The X-ray energy was calibrated using the spectrum of a Cu foil. Sample solutions were sealed in a flow cell (path length = 2 mm) with windows made of pyrolytically prepared boron nitride plates (150 μm, Shinetsu). The flow cell was covered with an aluminum jacket, in which the thermostated water at 25.0 ± 0.1 °C was circulated. The XAFS measurements in the transmission mode were carried out by the conventional arrangement of the ionization chambers and the sample cell. For the fluorescent XAFS measurements, the monochromatized X-ray was irradiated into a sample solution with an incident angle of 45°, and the fluorescent X-ray was monitored in the orthogonal direction of the irradiated X-ray. The undercounting of SSD was corrected according to the method reported.[36]

The background absorption in the pre-edge region was estimated by the Victoreen function for the XAFS spectra measured in the transmission mode. The fluorescent X-ray spectra of the solvent were independently measured and were subtracted from those of the sample solution by referring to the intensity of the incident X-ray to remove the background in the pre-edge region. The smooth background in the post-edge region was estimated by the cubic spline function to obtain the normalized EXAFS oscillation ($\chi(k)$) using the program REX (Rigaku).[37] The k^3-weighted $\chi(k)$ curves are shown in Figures S2 and S3 for all of the sample solutions measured in this study. The obtained $k^3\chi(k)$ values and the k^3-weighted theoretical function of the EXAFS oscillation expressed by eq 10 were converted in the R space for the optimization of the structure parameters by Fourier transformation using the Hanning-type window function with a width of 0.5 Å to determine the structure parameters.

$$\chi(k) = \sum_j \frac{F_j(k) S_{0,j}{}^2 N_j}{kR_j{}^2} \sin(2R_j k + \delta_j(k)) \exp\left(-2k^2\sigma_j{}^2 - \frac{2R_j}{\lambda_j(k)}\right) \quad (10)$$

where $F_j(k)$ is the scattering amplitude from each of the N_j scatterers at distance R_j from the X-ray absorbing atom, $\delta_j(k)$ is the total phase shift, $S_{0,j}{}^2$ is the dumping factor, $\lambda_j(k)$ is the mean free path of a photoelectron, and $\sigma_j{}^2$ is the mean square displacement of R_j. The values of $F_j(k)$, $\delta_j(k)$, and $\lambda_j(k)$ based on the crystal structures of $[Cu(tpp)]$[38] and $[Cu(an)_4(pz)](BF_4)_2$[39] for the interaction with the pyrrolenine group of the porphyrin and AN, respectively, were calculated using the program FEFF7.[40] For the Cu−O(water) interaction, the model structure with four Cu−O (1.94 Å) and two Cu−O (2.43 Å) interactions, which was constructed on the basis of the results of the X-ray diffraction, was used as the structural standard.[41,42] The nonlinear least-squares calculations were carried out by the program FEFFIT[43] in the R range

(30) Adler, A. D.; Longo, F. R.; Finarelli, J. D.; Goldmacher, J.; Assour, J.; Korsakoff, L. *J. Org. Chem.* **1967**, *32*, 476.
(31) Barfnett, G. H.; Hudson, M. F.; Smith, K. M. *J. Chem. Soc., Perkin Trans. 1* **1975**, 1401.
(32) Lindsey, J. S.; Wanger, R. W. *J. Org. Chem.* **1989**, *54*, 828.
(33) Suzuki, H.; Ishiguro, S. *Inorg. Chem.* **1992**, *31*, 4178.
(34) Nomura, M.; Koyama, A. KEK Report 95-15; National Laboratory for High Energy Physics, Tsukuba, 1996.
(35) Nomura, M. *J. Synchrotron Radiat.* **1998**, *5*, 851.
(36) Nomura, M. KEK Report 98-4; National Laboratory for High Energy Physics, Tsukuba, 1998.
(37) Teranishi, T.; Harada, M.; Asakura, K.; Asanuma, H.; Saito, Y.; Toshima, N. *J. Chem. Phys.* **1994**, *98*, 7967.
(38) Fleischer, E. B.; Miller, C. K.; Webb, L. E. *J. Am. Chem. Soc.* **1964**, *86*, 2342.
(39) Begley, M. J.; Hubberstey, P.; Stroud, J. *J. Chem. Soc., Dalton Trans.* **1996**, 2323.
(40) Zabinsky, S. I.; Rehr, J. J.; Ankudinov, A.; Albers, R. C.; Eller, M. *Phys. Rev. B* **1995**, *52*, 2995.
(41) Marcus, Y. *Chem. Rev.* **1988**, *88*, 1475.
(42) Ohtaki, H.; Radnai, T. *Chem. Rev.* **1993**, *93*, 1157.
(43) Newville, M.; Ravel, R.; Haskel, D.; Rehr, J. J.; Stern, E. A.; Yacoby, Y. *Phys. B* **1995**, *208/209*, 154.

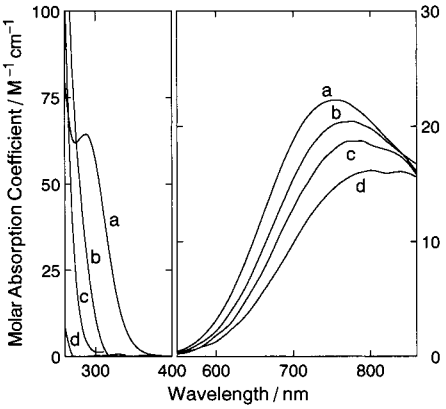

Figure 1. UV−vis absorption spectra of $[Cu(H_2O)_n(an)_{6-n}]^{2+}$ in aqueous acetonitrile. (a) $n = 0$, (b) $n = 1$, (c) $n = 2$, and (d) $n = 3$.

from 0.8 to 4.5 Å in the case of the Cu(II)−SAT complexes and from 0.8 to 3.0 Å in the case of $[Cu(H_2O)_n(an)_{6-n}]^{2+}$ to optimize the values of N_j, R_j, σ_j^2, and the correction of the edge energy (ΔE_0).

Kinetic Measurements. The spectral change for the reactions of H_2tpp, H_2t(4-Clp)p, H_2tmp, and H_2oep with the Cu(II) ion in aqueous AN was measured by a stopped-flow rapid detection system (RSP-801, Unisoku, Japan) in the wavelength range from 300 to 550 nm. The absorbance, A, was followed after mixing the aqueous AN solutions of the porphyrin and a large excess of the Cu(II) ion to determine the conditional first-order rate constant, k_{obs}, according to eq 11.

$$A = A_\infty - (A_\infty - A_0)\exp(-k_{obs}t) \tag{11}$$

where A_∞ and A_0 are the absorbance at $t = \infty$ and 0, respectively. The temperature of all of the measurements was maintained at 25.0 ± 0.1 °C using circulating thermostated water.

Results and Discussion

Formation Equilibria of $[Cu(H_2O)_n(an)_{6-n}]^{2+}$ Complexes in Acetonitrile. According to eqs 7−9, the values of β_n for the water addition reaction were determined at 298 K as follows: $\log(\beta_1/M^{-1}) = 1.19 \pm 0.18$, $\log(\beta_2/M^{-2}) = 1.86 \pm 0.35$, and $\log(\beta_3/M^{-3}) = 2.12 \pm 0.57$. The formation of the $[Cu(H_2O)_n(an)_{6-n}]^{2+}$ ($n > 3$) complexes was not observed under the present experimental conditions with C_W less than 0.9 M. The determined absorption spectra of the $[Cu(H_2O)_n(an)_{6-n}]^{2+}$ ($n = 0-3$) complexes are shown in Figure 1. The absorption band maximum (λ_{max}) of the d−d transition is 756 (the molar absorption coefficient = 22.7 M^{-1} cm^{-1}), 776 (20.4), 788 (18.7), and 800 (16.2) nm for $[Cu(an)_6]^{2+}$, $[Cu(H_2O)(an)_5]^{2+}$, $[Cu(H_2O)_2(an)_4]^{2+}$, and $[Cu(H_2O)_3(an)_3]^{2+}$, respectively. The red shift of λ_{max} with the increasing number of bound water molecules is identical to the corresponding series of $[Cu(dmf)_n(an)_{6-n}]^{2+}$ (dmf = *N*,*N*-dimethylformamide) in AN, for which the λ_{max} values are 772, 782, and 819 nm for $n = 1$, 2, and 3, respectively.[4] Because the substitution of the bound AN molecule having a stronger π-accepting property than water and dmf makes the ligand-field splitting of the Cu(II) ion small, it is reasonable that the λ_{max} value increases with the increasing number of water or dmf molecules bound to the Cu(II) ion.

Local Structure around the Cu(II) Ion in $[Cu(H_2O)_n(an)_{6-n}]^{2+}$ Complexes Formed in Acetonitrile. It is suggested by the UV−vis absorption spectra of the $[Cu(H_2O)_n(an)_{6-n}]^{2+}$ ($n = 0-3$) complexes shown in Figure 1 that the geometry around the Cu(II) ion is tetragonally distorted six-coordinate because of the d−d absorption band with tailing in the longer wavelength range than the absorption maximum.[44] This indicates that the AN molecules coordinate at the axial site of the Cu(II) ion. To determine the structure parameters around the Cu(II) ion in $[Cu(H_2O)_n(an)_{6-n}]^{2+}$, the XAFS spectra were measured for a variety of C_W values with almost a constant C_{Cu} of 0.1 M (see Table S2). The $k^3\chi(k)$ curves shown in Figure S2 were Fourier transformed in the k range from 2.0 to 14.0 $Å^{-1}$, and the absolute values of the Fourier transform magnitudes are depicted in Figure S4. The main peak at around 1.5−1.6 Å is attributed to the bonding interaction between the Cu(II) ion and the nitrogen atoms of AN or the oxygen atoms of water. The feature observed in the R range of 1.8−4.5 Å is considered to correspond to the nonbonding interactions between the Cu(II) ion and the carbon atoms of AN and to the multiple scattering, which is focused by the linear arrangement of the AN molecule toward the Cu(II) center.

Table 1. Structure Parameters around the Cu(II) Ion in the $[Cu(H_2O)_n(an)_{6-n}]^{2+}$ Complexes Formed in Acetonitrile[a]

	R/Å			$\sigma^2/10^{-2}$ Å^2		
complex	Cu−N_{eq}	Cu−N_{ax}	Cu−O_{eq}	Cu−N_{eq}	Cu−N_{ax}	Cu−O_{eq}
$[Cu(an)_6]^{2+}$	2.00	2.49		1.02	2.67	
$[Cu(H_2O)(an)_5]^{2+}$	2.00	2.48	1.96	0.86	2.89	1.04
$[Cu(H_2O)_2(an)_4]^{2+}$	2.01	2.52	1.95	0.75	2.89[b]	1.04[b]
$[Cu(H_2O)_3(an)_3]^{2+}$	1.98	2.38	1.97	0.75[b]	2.89[b]	0.84
$[Cu(H_2O)_6]^{2+}$[c]			1.97[d]			0.75[d]

[a] N_{eq}, N_{ax}, and O_{eq} refer to the nitrogen of AN at the equatorial site, the nitrogen of AN at the axial site, and the oxygen of water at the equatorial site, respectively. [b] Fixed during the least-squares calculation. [c] In water. [d] The R and σ^2 values of the Cu−O interaction at the axial site were 2.29 Å and 0.88 × 10^{-2} Å^2, respectively.

The observed $k^3\chi(k)$ values were first analyzed using eqs 8, 9, and 12 to estimate the β_n values.[45]

$$\chi_{obs}(k) = \frac{\sum_n \chi_{Cu(H_2O)_n}(k)\,[Cu(H_2O)_n(an)_{6-n}^{2+}]}{C_{Cu}} \tag{12}$$

where $\chi_{Cu(H_2O)_n}(k)$ is the $\chi(k)$ value of the component species of $[Cu(H_2O)_n(an)_{6-n}]^{2+}$. The obtained values of $\log(\beta_1/M^{-1}) = 1.1 \pm 0.8$, $\log(\beta_2/M^{-2}) = 1.3 \pm 1.0$, and $\log(\beta_3/M^{-3}) = 0.9 \pm 0.8$ were in excellent agreement with those determined by the UV−vis absorption spectroscopy within the experimental uncertainty. The Fourier transform magnitudes were then analyzed by fixing all of the N on the basis of the β_n values determined using the UV−vis absorption. The obtained structure parameters are listed in Table S4. The structure parameters of $[Cu(an)_6]^{2+}$ were determined using the EXAFS data of solution CW0 (see Table S2) because the amount of $[Cu(H_2O)_n(an)_{6-n}]^{2+}$ ($n > 0$) was negligible. Because both of the $[Cu(an)_6]^{2+}$ and $[Cu(H_2O)(an)_5]^{2+}$ complexes were contained in solutions CW1−CW3, the structure parameters of the latter were optimized by fixing those of the former. Similarly, the structure parameters of $[Cu(H_2O)_2(an)_4]^{2+}$ and $[Cu(H_2O)_3(an)_3]^{2+}$ were determined by the analysis of the EXAFS spectra of solutions CW4−CW6 and CW7−CW9, respectively. The optimized parameters of $[Cu(H_2O)_n(an)_{6-n}]^{2+}$ were in excellent agreement for the three solutions, respectively, and the averaged values of R and σ^2 are summarized in Table 1. The fitting results of solutions CW0, CW3, CW6, and CW9 are drawn in Figure S5. As seen in Figures S2 and S4, there is meaningful difference in the $k^3\chi(k)$ values and their Fourier transformations in response to the change in C_W. Because the multiple-scattering contribution in the case of the Cu−an interaction is emphasized by the linear

(44) Lever, A. B. P. *Inorganic Electronic Spectroscopy*, 2nd ed.; Elsevier: Amsterdam, 1984.
(45) Inada, Y.; Funahashi, S. *Z. Naturforsch.* **1999**, *54b*, 1517.

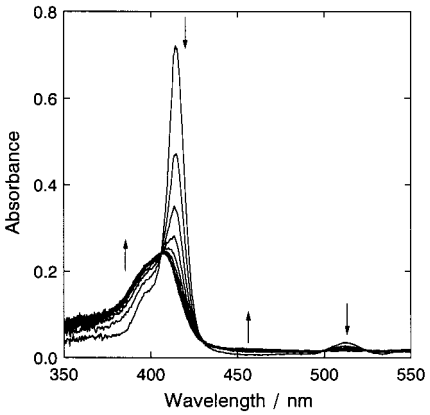

Figure 2. The change in the UV−vis absorption spectra for the reaction of H_2tmp with the Cu(II) species in aqueous acetonitrile. The values of C_{Cu} and C_W were 1.69×10^{-4} and 0.224 M, respectively. The initial concentration of H_2tmp was 1.6×10^{-6} M. The spectra at 0.1, 0.7, 1.3, 1.9, 2.5, 3.1, 3.7, 4.3, 4.9, and 5.5 s after the start of the reaction were depicted.

alignment of the AN molecule toward the Cu(II) center, the distinction between the Cu−H_2O and Cu−an interactions is possible by systematic measurements while changing the solution composition and the analysis in considering the multiple scattering.

The obtained Cu−O bond distance of $[Cu(H_2O)_6]^{2+}$ is consistent with those previously reported.[42,46] The *R* value of $[Cu(an)_6]^{2+}$ at the equatorial site is almost in agreement with those previously obtained from the XAFS spectra in the transmission mode.[2,47,48] Furthermore, this value is also comparable to that determined by the fluorescent XAFS measurement (vide infra), although the concentration of the Cu(II) ion (C_{Cu}) has a significant range of 2 orders of magnitude. This finding indicates that the structure around the Cu(II) ion is maintained over a wide range of C_{Cu}, and that the existence of the contact ion pair between the Cu(II) ion and $CF_3SO_3^-$ in AN is negligible up to a C_{Cu} value of at least 0.5 M. The *R* values of the Cu−N_{eq} and Cu−O_{eq} interactions are considered to be constant for a series of $[Cu(H_2O)_n(an)_{6-n}]^{2+}$ ($n = 0-3$ and 6), although a slight elongation was observed for a corresponding series of $[Cu(py)_n(an)_{6-n}]^{2+}$ ($n = 0-4$).[2] The different trend between water and py is ascribed to the stronger σ donating ability of py than that of water.

Characterization of the Cu(II)−SAT Complexes in Aqueous Acetonitrile. The Cu(II)−SAT complex was reported to form as a stable reaction product between H_2tpp and the Cu(II) ion in AN.[2,3] In the present study, the reactions of H_2t(4-Clp)p, H_2tmp, and H_2oep, in addition to H_2tpp, with the Cu(II) ion were investigated in aqueous AN to compare the reactivities of the porphyrins having various substituents. The change in the UV−vis absorption spectra for the reaction of H_2tmp is shown in Figure 2, and those of the other porphyrins are given in Figure S6. The spectral change in the case of H_2tpp is in perfect agreement with that reported in neat AN,[2,3] and it is concluded that the Cu(II)−SAT complex, $Cu(H_2tpp)^{2+}$, is also formed in aqueous AN. The spectral change of the other porphyrins is similar to that of H_2tpp, and the absorption spectra of the reaction products are apparently different from those of the corresponding metalloporphyrins [Cu(por)]. Furthermore, the addition of pyridine into the solution of the Cu(II)−SAT complex led to the formation of [Cu(por)] as shown in Figure S7. These results strongly indicate that the protons on the pyrrole nitrogen of the porphyrin still remain in the reaction products, and that they are dissociated by the reaction with pyridine. The product of the reaction between the Cu(II) ion and H_2por in aqueous AN is thus concluded to be the Cu(II)−SAT complex, $Cu(H_2por)^{2+}$. The absorption spectral data of the free base porphyrins (H_2por), the Cu(II)−SAT complexes ($Cu(H_2por)^{2+}$), and the metalloporphyrins ([Cu(por)]) in aqueous AN are tabulated in Table 2.

The wavelength of the main peak for the Soret band is in the order of H_2por > [Cu(por)] > $Cu(H_2por)^{2+}$ for three *meso*-substituted porphyrins (H_2tpp, H_2t(4-Clp)p, and H_2tmp). The Cu(II)−SAT complexes of the *meso*-substituted porphyrins are commonly characterized by the broad and blue-shifted Soret band relative to those of the corresponding free base porphyrin. The narrow and red-shifted Soret band revives when the remaining protons on the pyrrole nitrogens in the Cu(II)−SAT complex are released to form the metalloporphyrin (see Table 2 and Figure S7). On the other hand, the β-substituted porphyrin, H_2oep, has a broad and blue-shifted Soret band in comparison with those of the *meso*-substituted porphyrins, even in the free base form as shown in Figure S8. This may indicate that the porphyrin ring of H_2oep is fluctuated in solution and is easily distorted from the planar structure.

Structure of the Cu(II)−SAT Complexes Formed in Acetonitrile. To determine the structure parameters around the Cu(II) ion in $Cu(H_2por)^{2+}$, we have carried out the fluorescent XAFS measurements for H_2tmp and H_2oep. The fluorescent XAFS spectra of [Cu(t(4-Clp)p)] and [Cu(oep)] were also measured in pyridine for comparison. The observed $k^3\chi(k)$ values in Figure S3 were Fourier transformed for the *k* values between 2.0 and 14.5 Å^{-1}. The observed Fourier transform magnitudes for the Cu(II)−SAT complexes of H_2tmp and H_2oep are shown in Figure 3 together with the calculated curves using the optimized parameters, and the corresponding plots of [Cu(t(4-Clp)p)] and [Cu(oep)] are given in Figure S9. The calculated $k^3\chi(k)$ functions were given in Figure S3.

As pointed out previously,[5] a clear difference was observed in the Fourier transform magnitudes in the *R* range from 2 to 4 Å between the Cu(II)−SAT complex and the metalloporphyrin or $[Cu(an)_6]^{2+}$ (see Figure 2 in ref 5). This is also the present case for H_2oep and H_2tmp. This finding indicates that the interactions between the Cu(II) ion and the two kinds of nitrogens, that is, the pyrrolenine nitrogen of porphyrin and the nitrile nitrogen of solvent AN, can be resolvable by taking into consideration the multiple scatterings and the nonbonding interactions in the curve-fitting analysis of the EXAFS data.

The Fourier transform magnitudes of the Cu(II)−SAT complexes were analyzed by assuming the three-shell model around the Cu(II) ion, that is, the interaction between the Cu(II) ion and (1) pyrrolenine nitrogens of porphyrin (Cu−N(pyr)), (2) AN molecules at the equatorial site (Cu−$N(an)_{eq}$), and (3) AN molecules at the axial site (Cu−$N(an)_{ax}$), which is the same as that used in the analysis of the Cu(II)−SAT complex of H_2-tpp.[5] The *N* values of these interactions in the Cu(II)−SAT complexes were optimized, and the number of nitrogens bound to the Cu(II) ion in [Cu(por)] was fixed at 4. In addition to the analysis using the three-shell model, we also carried out the curve-fitting procedure using the two-shell model, in which the interaction with AN molecules at the axial site was excluded. The obtained structure parameters are given in Table S5. As is apparent from Table S5, the reproducibility of the Fourier

(46) Inada, Y.; Sugimoto, K.; Ozutsumi, K.; Funahashi, S. *Inorg. Chem.* **1994**, *33*, 1875.
(47) Funahashi, S.; Inada, Y. *Trends Inorg. Chem.* **1998**, *5*, 15.
(48) Persson, I.; Penner-Hahn, J. E.; Hodgson, K. O. *Inorg. Chem.* **1993**, *32*, 2497.

Table 2. Absorption Spectral Data of Free Base Porphyrins, the Cu(II)−SAT Complexes, and Metalloporphyrins in Aqueous Acetonitrile[a,b]

species	absorption peak maxima/nm	
	Soret band	Q band
H_2tpp	365[sh], 395[sh], 413 (5.68)	478 (3.54), 512 (4.28), 546 (3.92), 587 (3.76), 644 (3.67)
H_2t(4-Clp)p	370[sh], 396[sh], 415 (5.67)	480 (3.51), 512 (4.27), 546 (3.89), 588 (3.73), 645 (3.65)
H_2tmp	368[sh], 397[sh], 414 (5.65)	479 (3.47), 513 (4.27), 545 (3.75), 590 (3.75), 645 (3.60)
H_2oep	347[sh], 372[sh], 393 (5.21)	468[sh], 495 (4.16), 529 (4.05), 565 (3.87), 619 (3.79)
$[Cu(H_2tpp)(an)_4]^{2+}$	364[sh], 388[sh], 405 (5.15), 435[sh]	600 (3.90), 639 (4.08)
$[Cu(H_2t(4-Clp)p)(an)_4]^{2+}$	365[sh], 389[sh], 408 (5.17), 438[sh]	598 (4.27), 655 (4.28)
$[Cu(H_2tmp)(an)_4]^{2+}$	360[sh], 391[sh], 407 (5.27), 455[sh]	565[sh], 662 (4.30), 710 (4.24)
$[Cu(H_2oep)(an)_4]^{2+}$	348 (4.91), 379 [sh]	*c*
[Cu(tpp)]	391[sh], 411 (5.72)	538 (4.33), 574[sh]
[Cu(t(4-Clp)p)]	392[sh], 413 (5.71)	540 (4.92), 576[sh]
[Cu(tmp)]	393[sh], 414 (5.77)	512[sh], 539 (4.29)
[Cu(oep)]	374[sh], 394 (5.57)	521 (4.16), 558 (4.44)

[a] The superscript, "sh", means the shoulder. [b] Values in parentheses represent $\log(\epsilon/M^{-1}\ cm^{-1})$. [c] The clear peaks were not observed.

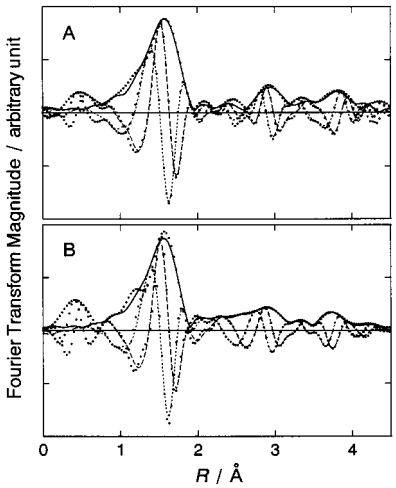

Figure 3. The observed and calculated Fourier transform magnitudes for the Cu(II)−SAT complexes of H_2tmp (A) and H_2oep (B). The observed values are represented by dots. The imaginary part, the real part, and the absolute value of the calculated magnitude are shown by the broken line, dotted line, and solid line, respectively.

transform magnitudes when using the three-shell model was better than that when using the two-shell model. Furthermore, the Cu···C_2 (C_2 is the methine carbon of the porphyrin) distance in all of the Cu(II)−SAT complexes was abnormally shorter for the two-shell model, rather than the corresponding distance in [Cu(por)]. Although the distorted porphyrin ring in the Cu(II)−SAT complex was supported by many evidences, such as UV−vis absorption spectrum and ^{1}H NMR spectrum,[2−5] the shortening of the Cu···C_2 distance in the Cu(II)−SAT complexes cannot be reasonably interpreted using any distorted frameworks of the porphyrin core. In the case of the results using the three-shell model, the Cu···C_2 distance was approximately comparable with that in the metalloporphyrin. Thus, the three-shell model is reasonable. The *R* values of the bonding interactions around the Cu(II) ion obtained using the three-shell model are summarized in Table 3. As shown in Figures 3 and S9, the depicted calculated curves using the obtained structure parameters reproduce the observed Fourier transform magnitudes well.

According to the structural analysis of the Cu(II)−SAT complexes, the Cu(II) ion is concluded to be bound by six nitrogens, that is, two pyrrolenine nitrogens (N(pyr)), two nitrogens of AN at the equatorial site ($N(an)_{eq}$), and two nitrogens of AN at the axial site ($N(an)_{ax}$) (see Table S5). The chemical formula of the Cu(II)−SAT complex in AN is thus described as $[Cu(H_2por)(an)_4]^{2+}$. The Cu−N(pyr) bond distance

Table 3. Distance of the Bonding Interactions in the Cu(II)−SAT Complexes, Metalloporphyrins, and $[Cu(an)_6]^{2+}$ in Acetonitrile

species	*R*/Å[a]		
	Cu−N(pyr)	Cu−$N(an)_{eq}$	Cu−$N(an)_{ax}$
$[Cu(H_2tpp)(an)_4]^{2+}$[b]	2.05	1.98	2.32
$[Cu(H_2tmp)(an)_4]^{2+}$[b]	2.03	1.96	2.45
$[Cu(H_2oep)(an)_4]^{2+}$	1.97	1.98	2.43
[Cu(tpp)][b,c]	2.02		
[Cu(t(4-Clp)p)][c]	2.02		
[Cu(oep)][c]	2.01		
$[Cu(an)_6]^{2+}$		1.99	2.40

[a] N(pyr) and N(an) represent the pyrrolenine or pyrrole nitrogen of porphyrin and nitrogen of AN, respectively. The subscripts, "eq" and "ax", mean the equatorial and axial sites of the Cu(II) ion, respectively. [b] Reference 5. [c] In pyridine.

(2.04 Å) of $[Cu(H_2tpp)(an)_4]^{2+}$ and $[Cu(H_2tmp)(an)_4]^{2+}$ for the *meso*-substituted porphyrins is slightly longer than that (2.02 Å) of [Cu(por)]. As pointed out in a previous paper,[5] the longer bond distance of Cu−N(pyr) is ascribed to the limitation due to the steric geometry of the porphyrin core, and the bite angle of N(pyr)−Cu−N(pyr) should be much greater than 90°, considering the bidentate coordination of the opposite two pyrrolenine groups, as indicated by the ^{1}H NMR spectrum of H_2tpp in the Cu(II)−SAT complex.[2] As is apparent from Table 3, the corresponding *R* values of the Cu−N(an) interactions for the three Cu(II)−SAT complexes are similar to each other, and they are almost identical with those in $[Cu(an)_6]^{2+}$. The bulkiness of the *meso*-substituents of the porphyrin appears to have no influence on the structure of the Cu(II)−SAT complex because the corresponding *R* values of $[Cu(H_2tmp)(an)_4]^{2+}$ and $[Cu(H_2tpp)(an)_4]^{2+}$ are almost identical. On the other hand, interestingly, the Cu−N(pyr) distance (1.97 Å) of the Cu(II)−SAT complex of the β-substituted porphyrin ($[Cu(H_2oep)(an)_4]^{2+}$) is significantly shorter than the corresponding distance (2.01 Å) of [Cu(oep)]. The shorter bond distance may suggest the flexibility of the porphyrin ring of H_2oep.

The *R* values for the various interactions in [Cu(por)] (por = tpp, t(4-Clp)p, and oep) are identical regardless of the different positions of the substituents (see Table 3). The N(pyr)−Cu−C_2 (C_2 = the methine carbon of the porphyrin) angle is calculated to be ca. 45° for these porphyrins using the intramolecular N(pyr)−C_1 (C_1 = the α carbon of the pyrrolenine or pyrrole group) and the C_1−C_2 bond lengths in a single crystal of [Cu(tpp)].[38] The Cu(II) ion is thus just incorporated into the porphyrin core, and the component atoms of the porphyrin ring are almost coplanar for the three [Cu(por)] in AN. All of the *R* values of [Cu(por)] determined in this study are longer by 2−5 pm than the corresponding bond length (1.98−2.01 Å) in the

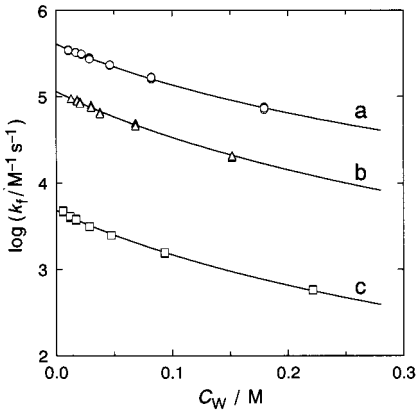

Figure 4. The k_f values plotted as a function of C_W in aqueous acetonitrile at 298 K for H_2tpp (a), H_2t(4-Clp)p (b), and H_2tmp (c).

single crystal.[38] This finding may indicate that the porphyrin ring of [Cu(por)] in AN is bloated due to the interaction between [Cu(por)] and the AN solvent molecules.

Formation Kinetics of the Cu(II)−SAT Complexes in Aqueous Acetonitrile. The reaction rates of the Cu(II)−SAT complex formation were measured under the conditions where the Cu(II) ion existed in a large excess over the porphyrin. The change in absorbance was first-order with respect to the porphyrin. The conditional first-order rate constants, k_{obs}, were then determined using eq 11 and were found to be proportional to C_{Cu} in the presence of the constant concentration of water, C_W, as shown in Figure S10. Because there is no intercept on the plot of k_{obs} versus C_{Cu}, the formation of the Cu(II)−SAT complex is quantitative, and the formation constant can be estimated to be larger than 10^7 M^{-1}. The second-order rate constant, k_f, which is defined as $k_f = k_{obs}/C_{Cu}$, was then determined by varying C_W. In the case of H_2oep, the reaction was too fast to be followed by the stopped-flow technique, but the k_f value for H_2oep was estimated to be greater than 1.5×10^6 M^{-1} s^{-1} according to the dead time (ca. 2 ms) of the rapid-mixing instrument used in this study. The obtained k_f values plotted as a function of C_W in Figure 4 are found to decrease with the increasing C_W. The dependence of k_f on C_W was then analyzed by taking into consideration the contribution of $[Cu(H_2O)(an)_5]^{2+}$ in addition to $[Cu(an)_6]^{2+}$, as shown in eqs 13 and 14.

$$H_2por + [Cu(an)_6]^{2+} \xrightarrow{k_{S0}} [Cu(H_2por)(an)_4]^{2+} + 2AN \quad (13)$$

$$H_2por + [Cu(H_2O)(an)_5]^{2+} \xrightarrow{k_{S1}} [Cu(H_2por)(an)_4]^{2+} + H_2O + AN \quad (14)$$

where k_{S0} and k_{S1} are the second-order rate constants for reactions 13 and 14, respectively. Because there was no difference in the absorption spectra of the Cu(II)−SAT complex formed under the conditions with a large variety of C_W, the water molecule bound to the Cu(II) ion in $[Cu(H_2O)(an)_5]^{2+}$ is considered to be released in the Cu(II)−SAT complex. Under the present experimental conditions with a large excess of C_{Cu} and C_W relative to the initial concentration of the porphyrins, the k_{obs} value is given by eq 15.

$$k_{obs} = k_{S0}[Cu(an)_6^{2+}] + k_{S1}[Cu(H_2O)(an)_5^{2+}] \quad (15)$$

In this equation, it is postulated that the substitution reaction of the coordinated AN and water molecules around the Cu(II) ion is much faster than that of the Cu(II)−SAT complex formation. The concentration of each Cu(II) species was calculated by eqs 8 and 9 using the β_n ($n = 1-3$) values, and the values of k_{S0} and k_{S1} were determined, as listed in Table 4, by a least-squares calculation of the k_{obs} values as a function of C_{Cu} and C_W. As shown in Figure 4, the calculated curves of k_{obs} using the obtained k_{S0} and k_{S1} values reproduced the observed data well. The reproducibility of the k_{obs} values was not improved by adding the contribution of the other Cu(II) species, such as $[Cu(H_2O)_2(an)_4]^{2+}$ and $[Cu(H_2O)_3(an)_3]^{2+}$. This means that the second-order rate constants of the Cu(II)−SAT complex formation for $[Cu(H_2O)_2(an)_4]^{2+}$ and $[Cu(H_2O)_3(an)_3]^{2+}$ are by far smaller in comparison with k_{S0} and k_{S1}.

Table 4. Second-Order Rate Constants, k_{S0} and k_{S1}, for the Formation of the Cu(II)−SAT Complexes in Aqueous Acetonitrile[a]

porphyrin	k_{S0}/M^{-1} s^{-1}	k_{S1}/M^{-1} s^{-1}
H_2tpp	$(4.1 \pm 0.2) \times 10^5$	$(3.6 \pm 0.2) \times 10^4$
H_2t(4-Clp)p	$(1.15 \pm 0.06) \times 10^5$	*b*
H_2tmp	$(4.8 \pm 0.3) \times 10^3$	$(1.3 \pm 0.3) \times 10^2$
H_2oep[c]	$>1.5 \times 10^6$	

[a] $T = 298$ K. [b] The k_{S1} value cannot be determined due to the error of measurements under the present experimental conditions. [c] The estimated value as the lower limit.

The rate of the SAT complex formation depends on the porphyrin structure in the order of H_2oep $\gg$ H_2tpp $>$ H_2t(4-Clp)p $\gg$ H_2tmp. The difference in the reactivity can be interpreted by the electronic and steric factors. The correlation between the porphyrin reactivity and the reduction potential of the porphyrins was explored. The faster metalloporphyrin formation reaction was observed for the porphyrin with a more negative reduction potential for the zinc(II) ion incorporation reaction into the water-insoluble porphyrins.[49,50] The reduction potentials parallel the basicity scale of the porphyrins, and thus the porphyrin bearing stronger basicity reacts with the zinc(II) ion faster than the less basic porphyrins.[49] Such a similar correlation, as shown in Figure S11, is observed in the present SAT complex formation reaction, except for H_2tmp which exhibits the steric effect on the reaction as mentioned below. The electron-withdrawing chlorine atoms on the *meso*-substituted phenyl groups may lower the electron density on the pyrrolenine nitrogen of H_2t(4-Clp)p, which is the first donating atom toward the Cu(II) ion during the Cu(II)−SAT complex formation. Because the outer-sphere association (eq 2) between the deformed porphyrin and the Cu(II) ion prior to the Cu(II)−SAT complex formation is considered to be driven by an electrostatic attraction between the local negative charge on the pyrrolenine nitrogens and the positive charge of the Cu(II) ion, the K_{OS} value should decrease due to the lower electron density for H_2t(4-Clp)p relative to H_2tpp. Furthermore, the rate-determining interchange reaction (eq 3) on the Cu(II) ion between the bound AN molecule and the incoming pyrrolenine nitrogen is also reduced by the lower electron density. The smaller k_{S0} value of H_2t(4-Clp)p than that of H_2tpp is thus ascribed to both the smaller K_{OS} value and smaller k_1 value as anticipated for the porphyrin containing the electron-withdrawing chlorine atoms.

In the case of the β-substituted porphyrin, H_2oep, the formation of the Cu(II)−SAT complex is very fast. This could

(49) Worthington, P.; Hambright, P.; Williams, R. F. X.; Reid, J.; Burnham, C.; Shamim, A.; Turay, J.; Bell, D. M.; Kirkland, R.; Little, R. G.; Datta-Gupta, N.; Eisner, U. *J. Inorg. Biochem.* **1980**, *12*, 281.
(50) Hambright, P. In *The Porphyrin Handbook*; Kadish, K. M., Smith, K. M., Guilard, R., Eds.; Academic Press: New York, 2000; Vol. 3, p 129.

be due to the greater flexibility of the porphyrin core of H_2oep as well as its higher basicity. As seen from the absorption spectrum of the free base form and the structure parameters of the Cu(II)−SAT complex (vide supra), the porphyrin ring of H_2oep is much more flexible than those of the *meso*-substituted porphyrins, and thus the energetic loss in the deformation process of the porphyrin ring (eq 1) during the Cu(II)−SAT complex formation is expected to be much smaller for the *β*-substituted porphyrin. To provide insight into the effect of the peripheral substituent groups on the flexibility of the porphyrin core, Scheidt et al. investigated the porphyrin molecular flexibility on the basis of the molecular structure of the porphyrin diacid species, H_4oep^{2+}, H_4tpp^{2+}, and H_4tmp^{2+} and the molecular mechanics calculations.[51] In this approach, a constant structural perturbation to the porphyrin molecules was provided by protonating the porphyrin free bases. It is known that the two unsubstituted pyrrolenic nitrogens can be protonated to afford dicationic porphyrin derivatives, H_4por^{2+}, with a strongly distorted D_{2d}-saddled conformation. The calculated barrier (0.55 kcal mol^{-1}) of H_4oep^{2+} to conformational inversion between the pair of D_{2d} isomers is smaller than that of H_4tpp^{2+} (1.0 kcal mol^{-1}). It was then concluded that the porphyrin with bulkier peripheral substituents has a less flexible porphyrin core. It is expected that this trend should reflect the flexibility of the free base porphyrin core, and in fact, it parallels the reactivity of the Cu(II)−SAT complex formation for H_2oep, H_2tpp, and H_2tmp in the present study. The fact that the rate constant for the Cu(II)−SAT complex formation of H_2oep is extremely large can be attributed to the higher flexibility of H_2oep which leads to the larger value of K_D.

The k_{S0} value for H_2tmp is by ca. 2 orders of magnitude smaller than that of H_2tpp, although the basicity of H_2tmp seems to be higher than H_2tpp judging from Figure S11. Similarly, a lower value for H_2tmp is observed for k_{S1}. This slowness should come from the steric hindrance due to the α-methyl groups of the *meso*-phenyl substituents of H_2tmp during the reaction with $[Cu(an)_6]^{2+}$ or $[Cu(H_2O)(an)_5]^{2+}$. The *meso*-phenyl rings of H_2tmp become more perpendicular to the porphyrin skeleton due to the steric interaction between the *o*-substituents on the phenyl rings and the hydrogen atoms on the pyrrole rings. The electrostatic approach between the Cu(II) ion and the deformed H_2tmp (eq 2) is thus inhibited by this steric effect. Furthermore, the K_D value for H_2tmp is considered to be much smaller than that for H_2tpp, because the H_2tmp molecule should be deformed to a greater extent rather than H_2tpp to effectively interact with the Cu(II) ion in the course of the Cu(II)−SAT complex formation. Because of the bulky substituents of H_2tmp, the more distant rupture in the bonding between the Cu(II) ion and the dissociating AN molecule is also required, and it is hard for the pyrrolenine nitrogen to closely approach the Cu(II) ion in the transition state. As described above, the observed trends in the rate constants of the Cu(II)−SAT complex formation for the *meso*-substituted porphyrins are satisfactorily interpreted on the basis of the proposed reaction mechanism of the Cu(II)−SAT complex formation as expressed by eqs 1−4. The schematic diagram of the reaction mechanism is also shown in Scheme 2.

The k_{S0} value for H_2tpp in aqueous AN is in accordance with that (3.6×10^5 M^{-1} s^{-1}) previously determined in neat AN.[2] The findings that the k_{S1} values for H_2tpp and H_2tmp are smaller than the respective k_{S0} values are consistent with the previous results using pyridine instead of water. Such a difference in the rate constant can be attributed to the decrease in the frequency of the intramolecular ax−eq interconversion on the Cu(II) ion, although the exchange rate of a bound solvent is generally accelerated by the coordination of electron donors,[52−55] such as pyridine and water. The almost parallel decrease in k_{S1} relative to the corresponding k_{S0} for H_2tpp and H_2tmp suggests that the formation mechanism of the Cu(II)−SAT complex for $[Cu(an)_6]^{2+}$, as expressed by eqs 1−4, is adoptable for the corresponding reaction for $[Cu(H_2O)(an)_5]^{2+}$. Interestingly, the k_{S1} value for H_2tpp obtained in this study is in good agreement with the corresponding value (3.5×10^4 M^{-1} s^{-1}) of $[Cu(py)(an)_5]^{2+}$ previously reported,[2] although the electron-donating ability of a bound water at the equatorial site of the Cu(II) ion is much poorer than that of pyridine. The deformation of H_2tpp (K_D) and the outer-sphere association (K_{OS}) between

Scheme 2

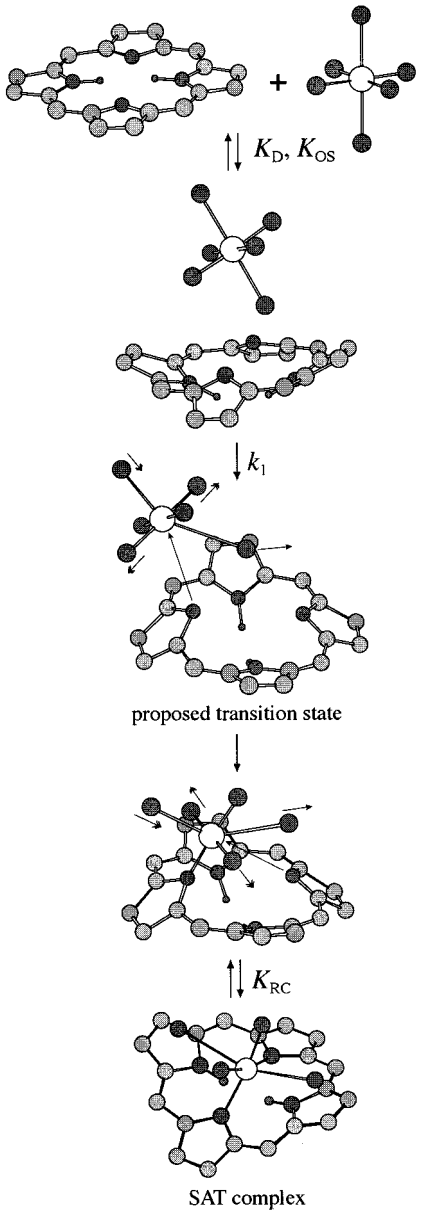

(51) Cheng, B.; Munro, O. Q.; Marques, H. M.; Scheidt, W. R. *J. Am. Chem. Soc.* **1997**, *119*, 10732.

(52) Hioki, A.; Funahashi, S.; Tanaka, M. *Inorg. Chem.* **1986**, *25*, 2904.
(53) Ishii, M.; Funahashi, S.; Tanaka, M. *Inorg. Chem.* **1988**, *27*, 3192.
(54) Mizuno, M.; Funahashi, S.; Nakasuka, N.; Tanaka, M. *Inorg. Chem.* **1991**, *30*, 1550.
(55) Cusanelli, A.; Frey, U.; Richens, D. T.; Merbach, A. E. *J. Am. Chem. Soc.* **1996**, *118*, 5265 and references therein.

the deformed H_2tpp and the Cu(II) species are considered to be identical for $[Cu(H_2O)(an)_5]^{2+}$ and $[Cu(py)(an)_5]^{2+}$. Thus, if the exchange rate of a bound AN molecule at the axial site of the Cu(II) ion is different between $[Cu(H_2O)(an)_5]^{2+}$ and $[Cu(py)(an)_5]^{2+}$, the respective k_{S1} values must be different from each other. It is then concluded that the dissociation rate of a bound AN at the axial site is not affected by the bound ligand at the equatorial site of the Cu(II) ion.

Acknowledgment. This work was supported by Grants-in-Aid for Scientific Research (Nos. 10440221, 10740305, 10874081, 11354009, and 11554030) from the Ministry of Education, Science, Sports, and Culture of Japan and by the REIMEI Research Resources of the Japan Atomic Energy Research Institute. The XAFS measurements were performed under the approval of the Photon Factory Program Advisory Committee (Proposal No. 97G054).

Supporting Information Available: Concentrations of sample solutions (Tables S1−S3), structure parameters for the sample solutions containing $[Cu(H_2O)_n(an)_{6-n}]^{2+}$ (Table S4), structure parameters of the Cu(II)−SAT complexes and some related compounds (Table S5), observed UV−vis absorption spectra of the Cu(II) ion in aqueous AN (Figure S1), observed EXAFS oscillations (Figure S2 and S3), Fourier transform magnitudes (Figure S4) and their fitting features (Figure S5) of the solutions containing $[Cu(H_2O)_n(an)_{6-n}]^{2+}$, change in the UV−vis absorption spectra of the Cu(II)−SAT complex formation for H_2tpp, H_2t(4-Clp)p, and H_2oep (Figure S6), spectral change by the addition of py into the solution of the Cu(II)−SAT complex (Figure S7), UV−vis absorption spectra of free base porphyrins (Figure S8), Fourier transform magnitudes of [Cu(t(4-Clp)p)] and [Cu(oep)] (Figure S9), Cu(II) ion concentration dependence of the conditional first-order rate constant of the SAT complex formation (Figure S10), and the correlation between the rate constant of the SAT complex formation reaction and the reduction potential of the free base porphyrin (Figure S11). This material is available free of charge via the Internet at http://pubs.acs.org.

IC010162B